Appl Phys B (2012) 106:921–926
DOI 10.1007/s00340-011-4811-x

Applied Physics B
Lasers and Optics

Direct determination of the dissociation probability in highly focused IR multiple photon dissociation

N.D. Gómez · V. D'Accurso · J. Codnia · F.A. Manzano · M.L. Azcárate

Received: 8 July 2011 / Revised version: 3 October 2011 / Published online: 26 November 2011

Abstract Laser-induced fluorescence (LIF) has been used to directly determine the dissociation probability per pulse in highly focused infrared multiple-photon dissociation (IRMPD). The fluence dependence of $CDCl_3$ IRMPD has been determined by LIF and FTIR spectrometry. The particular LIF irradiation and detection system's geometry implemented allowed us to monitor the local CCl_2 radicals concentration in the intersection zone of the observation and the dissociation volumes. The fluence dependence of the LIF intensity was modeled with the cumulative log-normal distribution. The dependence of the global values of the fraction of molecules dissociated per pulse on fluence was obtained from FTIR spectrometry. The dissociation probabilities per pulse were derived from the deconvolution of these values using the cumulative log-normal distribution. A very good agreement between the values of the parameters σ and Φ_{sat} obtained from the deconvolution technique with those resulting from the fluorescence intensity fit was found, showing the validity of the method proposed.

Carrera del Investigador de CONICET.

N.D. Gómez · V. D'Accurso · J. Codnia · F.A. Manzano · M.L. Azcárate (✉)
Centro de Investigaciones en Láseres y Aplicaciones (CEILAP), CITEDEF-CONICET, J.B. de La Salle 4397 (B160ALO), Villa Martelli, Argentina
e-mail: lazcarate@citedef.gob.ar
Fax: 54-11-47098100

N.D. Gómez
e-mail: ndgomez@citedef.gob.ar

V. D'Accurso
e-mail: vdacurso@citedef.gob.ar

J. Codnia
e-mail: jcodnia@citedef.gob.ar

F.A. Manzano
e-mail: fmanzano@citedef.gob.ar

1 Introduction

Infrared multiple-photon dissociation (IRMPD) is a widely spread technique used in vibrational photochemistry studies and laser isotope separation [1–3]. An important parameter is the dissociation probability which depends on the laser energy per unit area or fluence. Small and medium size molecules are often characterized by high dissociation energy thresholds. Therefore, focused laser beams are usually employed to obtain high fluences to attain dissociation. As a consequence, there is a strong variation of the fluence in the photolysis volume. Given that in highly focused geometries the effective volumes are very small, usually a large number of irradiation pulses is required to obtain appreciable dissociation yields. With low repetition rate lasers, the experiments last several hours. The global dissociation yield can be described in terms of an effective volume since the fraction of molecules dissociated per pulse in the irradiated volume is diluted in the whole cell volume. Global values of the dissociation yield can be obtained from infrared spectrometry. In addition, deconvolution procedures must be used to obtain the fluence dependence of the dissociation probability. Several deconvolution models have been proposed [4–12]. However, a two-parameter model based on the cumulative log-normal distribution has demonstrated to satisfactorily describe the dissociation probabilities of molecules over a wide fluence range in IRMPD [10–12]. In view of these considerations, a technique that would permit the direct determination of the dissociation probability in focused geometries would be very advantageous and time saving.

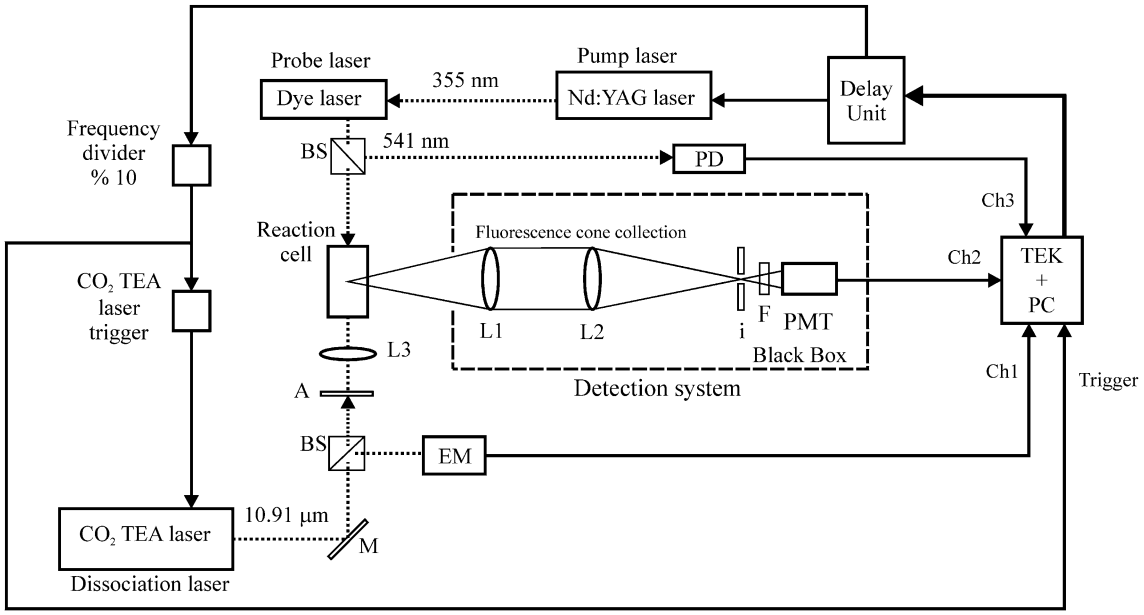

Fig. 1 Experimental setup. EM: energy meter, L1, L2: quartz lenses, L3: ZnSe lens, BS: beam-splitters, A: attenuators, TEK: digital oscilloscope with incorporated PC, PMT: photomultiplier, F: filter, i: iris, PD: photodiode, M: Mirror

Laser-induced fluorescence (LIF) is a highly selective and sensitive technique [13]. Molecules or reaction intermediates excited to an electronic excited state by resonant absorption of photons from a laser emit fluorescence on their decay to a lower level. The LIF technique can be used to monitor in real-time the fragments produced in highly focused IRMPD systems. The detection system's geometry can be arranged to "see" the fluorescence of the species in an irradiation region smaller than the focal volume of the photolysis laser [14]. Then, the photolysis can be considered to occur in a uniform beam geometry, in which case, the LIF signal values could be associated to the dissociation probability.

In this work we have used LIF to directly determine the dissociation probability per pulse in IRMPD. LIF and FTIR spectrometry have been used to determine the fluence dependence of $CDCl_3$ IRMPD which occurs mainly via the DCl elimination channel [15]:

$$CDCl_3 \longrightarrow CCl_2 + DCl \quad (1)$$

The particular LIF detection system's geometry implemented in this work allowed us to monitor the local CCl_2 radicals concentration in the intersection zone of the observation and the dissociation volumes. The fluence dependence of the LIF signal was modeled with the cumulative log-normal distribution.

Additionally, the dependence of the global values of the fraction molecules dissociated per pulse on the fluence was obtained from FTIR spectrometry. The deconvolution of these values to obtain the dissociation probabilities was performed using the cumulative log-normal distribution. The molecular parameters obtained coincide within experimental error with those derived from the LIF signal modeling. We have thus demonstrated that the irradiation and LIF detection system's geometry implemented enabled us to obtain the dissociation probabilities in highly focused IRMPD in a direct manner.

2 Experimental

The experimental setup is shown in Fig. 1. A homemade multimode, pulsed, tunable TEA CO_2 laser with an output average energy of 1.8 J at 1 Hz and 80 ns FWHM pulse length was used as IR radiation source for $CDCl_3$ IRMPD. The laser was tuned to the 10P(48), 916.7 cm^{-1}, emission line which is resonant with the $CDCl_3$ ν_4 vibrational mode (913.9 cm^{-1}) [16]. The laser radiation was focused into the center of the photolysis cell with a 9.4 cm focal length ZnSe lens. The laser energy was varied combining CaF_2 and BaF_2 flats of different thickness which allowed transmission factors between 1% and 80% so that the fluence in the center of the cell varied in the 3–400 J cm^{-2} range.

The CCl_2 radicals generated in the IRMPD of $CDCl_3$ were excited to the first electronic state with a home-made dye laser pumped by a frequency tripled Nd:YAG laser pulsed at a repetition rate of 10 Hz. The dye laser was tuned to 541 nm, resonant with a rotational-vibrational band of the CCl_2 A^1B_1 state. The laser pulse energy was 0.2 mJ, the pulse width FWHM was 3.5 ns and the beam diameter was 2 mm.

The lasers were externally synchronized with a delay unit, Stanford Research Systems DG 535, and entered into the reaction cell in a colinear way through opposite windows. The delay unit output used to trigger the TEA CO_2 laser was connected to the entrance of a frequency divider so as to obtain a repetition rate of 1 Hz. The fluorescence signal was detected at 90°. A system of two lenses of 9.5 cm and 24 cm focal lengths was used to collimate and focus the signal on an iris placed at the entrance of a photomultiplier tube, RCA 1P28. A wavelength longpass interference filter was disposed between the iris and the photomultiplier tube to diminish the background signal produced by the dye laser scattering in the reaction cell.

Data acquisition and processing and experiments' automation programs were developed. The lasers output energies were monitored from the beams reflections on different beam-splitters. The fluorescence signals as well as the CO_2 and dye lasers energies were acquired with an oscilloscope, Tektronix DPO 7054, for each dissociation laser pulse. For each pulse, the fluorescence intensity was determined from the maximum of the LIF signal normalized to the dye laser energy. For each fluence value, the LIF intensity signal was determined as the average of the intensities recorded for each dissociation laser pulse.

The experiments were performed at room temperature in a cylindrical Pyrex glass cell 2.75 cm diameter and 10 cm long sealed with NaCl and BaF_2 windows for the CO_2 and dye laser radiation transmission, respectively, and quartz for the fluorescence transmission. The $CDCl_3$ pressure was fixed at 1 Torr. $CDCI_3$ 99.98% provided by Merck was handled in a high-vacuum system with a turbomolecular pump (Leybold, Turbovac) pumped by a rotary vane pump (Leybold, Trivac) and purified through thaw-freeze cycles.

The number of irradiation pulses for each fluence value was chosen so that the global fraction of dissociated molecules was less than 10% in order to avoid interference from the products. The $CDCl_3$ pressure before and after irradiation with certain pulse numbers was determined by IR spectrometry with a FTIR spectrometer (Perkin-Elmer, System 2000) using a standard spectrum and a program based on non-linear regression techniques. In order to improve the signal-to-noise ratio, each spectrum was obtained from 40 scans registered with a resolution of 1 cm^{-1}.

3 Results

The local and global fractions of $CDCl_3$ molecules dissociated per pulse were characterized by laser-induced fluorescence (LIF) and FTIR spectrometry techniques, respectively. The irradiation and fluorescence detection scheme is shown in Fig. 2, where z and x indicate the coordinates in the laser pulse propagation and detection directions, respectively. The fluorescence observation region, shown as a dark cylinder in the center of the cell, was controlled by varying the iris aperture. An observation cylinder of $D = 3$ mm diameter and 9 mm length (field depth) was defined by fixing the iris diameter in 7 mm.

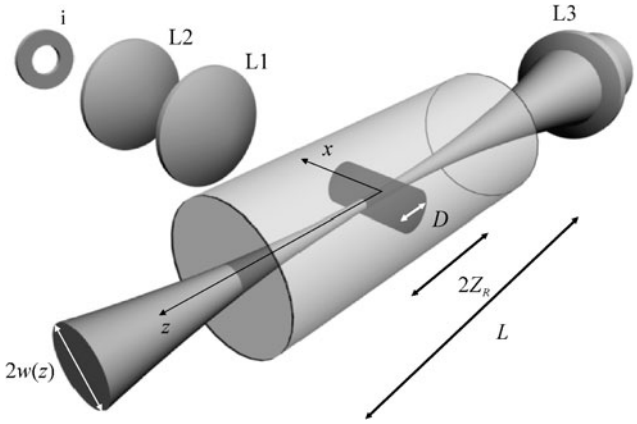

Fig. 2 Irradiation geometry and observation volume. Z_R: Rayleigh range, $2w$: beam's diameter; L1, L2: Quartz lenses; L3: ZnSe lens, D: observation region diameter, L: cell's length, i: iris

First, the laser spot size at the lens' focus was measured in order to determine the TEA CO_2 laser fluence. The integrated beam energy profile was measured by scrolling a razor blade placed on a translation stage with a micrometric screw and partially blocking the beam path (Fig. 3). Since the laser was multimode, a circular *top-hat* transverse energy distribution was used to model the results:

$$\Phi(r,z) = \begin{cases} \left(\frac{w_0}{w(z)}\right)^2 \Phi_0, & r \le w(z), \\ 0, & r > w(z), \end{cases} \tag{2}$$

with

$$w(z) = w_0 \sqrt{1 + \left(\frac{z}{Z_R}\right)^2}, \tag{3}$$

where Φ_0 and w_0 are the fluence and the laser beam waist at the focus, respectively, and Z_R is the Rayleigh range. The beam spot size at the lens' focus obtained was $w_0 = (0.37 \pm 0.02)$ mm.

Then, the Rayleigh range, Z_R, was determined from the beam diameters derived from the image processing of the beam imprints on thermosensitive paper at different distances from lens L3. A value of $Z_R = (3.6 \pm 0.3)$ mm was obtained from the fit with (3) of the data shown in Fig. 4. Given that the 3 mm observation region diameter (Fig. 2) is smaller than twice the Z_R value (7.2 mm), the fluence in the observation region can be considered constant. This assumption leads to an error in the mean fluence value determination less than 10%. We therefore assume that the LIF signal detected is related to the fraction of molecules dissociated per pulse in a region of constant fluence.

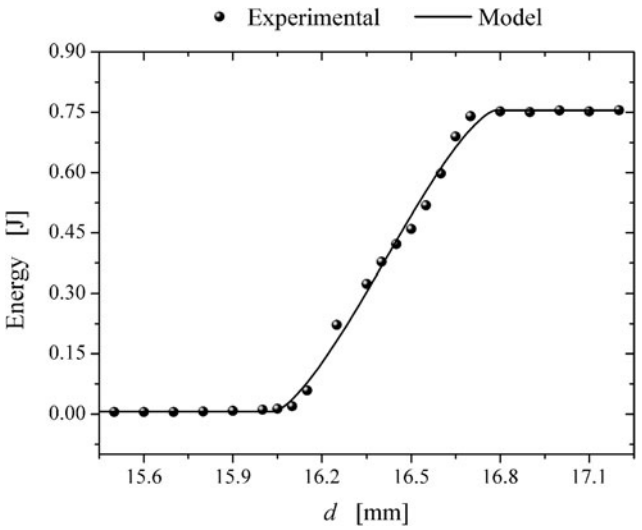

Fig. 3 Dependence of the integrated beam energy on the position of the razor blade

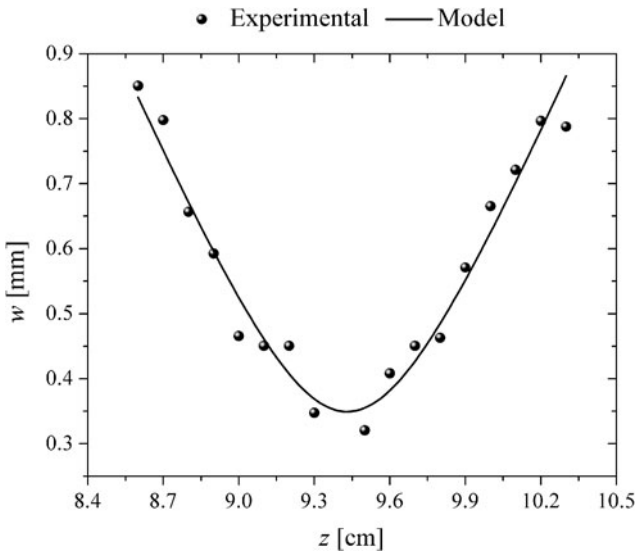

Fig. 4 Dependence of the beam imprint radius on thermosensitive paper on the lens distance

The maximum value of the LIF signal for each CO_2 laser pulse was used as an estimator of the fluorescence intensity. These maximum values were first normalized to the intensity of the dye laser to compensate for fluctuations and then averaged. In order to improve the signal-to-noise ratio, about 50 LIF signals were acquired for each fluence value.

Figure 5 shows the dependence of the average values of the maximum of the LIF signal on the fluence at the focus, Φ_0, in the 3–400 J cm^{-2} range. Two well differentiated regimes can be observed: a rise and a saturation regime. In the range between 3 and 20 J cm^{-2}, the fluorescence intensity increases approximately 3 orders of magnitude. At larger fluences a saturation regime is attained.

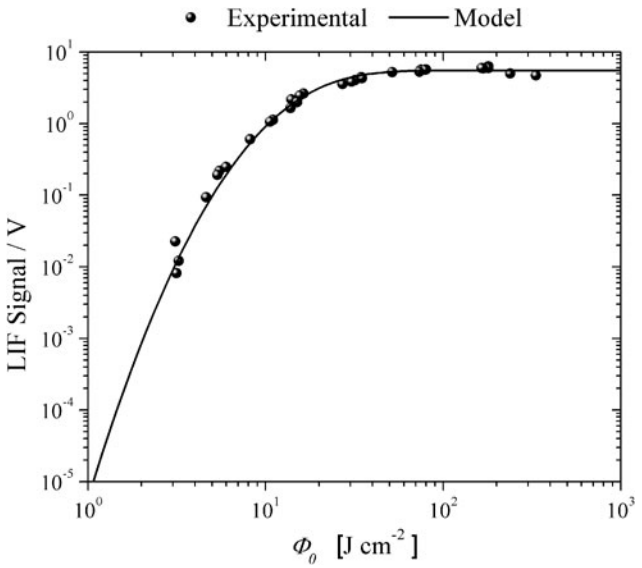

Fig. 5 Dependence of the LIF intensity on the fluence at the focus

Barker et al. [10–12] solved an energy-grained master equation to describe the IR multiple-photon dissociation process in polyatomic molecules and found that the fraction of molecules dissociated per pulse could be described assuming a Cumulative Log-Normal Distribution Function, CLNDF, for the dissociation probability per pulse as indicated in the equation

$$f(\Phi) = \frac{1}{2}\left[1 + \mathrm{erf}\left(\frac{\ln(\eta)}{\sqrt{2}\sigma}\right)\right], \tag{4}$$

where

$$\eta = \frac{\Phi}{\Phi_{\mathrm{sat}}}. \tag{5}$$

The parameter σ describes the f increase rate in the low fluence regime, while Φ_{sat} establishes a boundary between the low fluence regime, in which f increases monotonously, and the high fluence regime, in which the probability tends to saturation. These parameters depend on the molecule, and, particularly, the last one depends on the total sample pressure and establishes the dissociation threshold of the molecule. Barker's model is widely used in the IR multiple-photon dissociation processes analysis since it is more accurate than the power law and the exponential models [9].

A very good fit of the fluence dependence of the fluorescence intensity with (4) is shown in solid line in Fig. 5. The parameters values $\sigma = 0.60 \pm 0.02$ and $\Phi_{\mathrm{sat}} = (18 \pm 1)$ J cm^{-2} were obtained from this fit. The saturation fluence corresponds to the fluence value for which half the $CDCl_3$ molecules within the observation region are dissociated. The value of Φ_{sat} obtained is consistent with the values reported by other authors in different experimental conditions [17, 18]. The excellent agreement between the

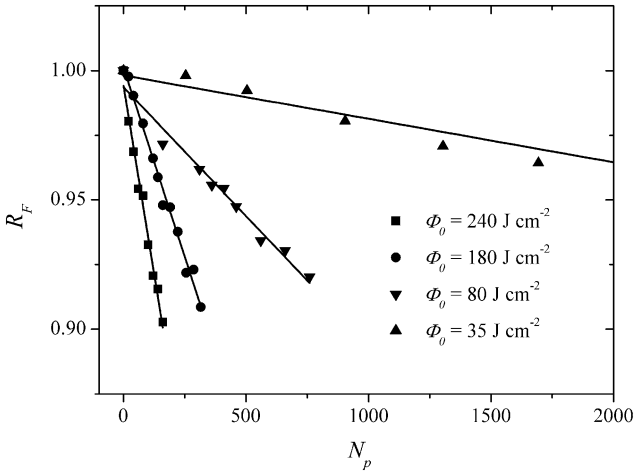

Fig. 6 Pulse number dependence of the $CDCl_3$ remnant fraction

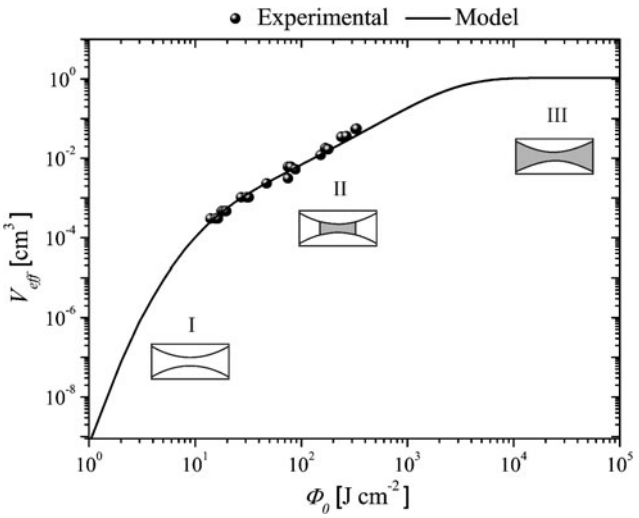

Fig. 7 Fluence dependence of the effective volume of dissociation. *Shaded areas* indicate regions with $\Phi > \Phi_{\mathrm{sat}}$

experimental values of the fluorescence intensity and the calculated values of the dissociation probability per pulse would indicate that the LIF signals are a direct measurement of the dissociation probabilities in highly focused geometries.

In order to prove this hypothesis, we carried out experiments to determine the global dissociation probability per pulse from the measurement of the fraction of molecules dissociated per pulse by infrared spectrometry.

In this case, the effective volume, defined as the volume in which the dissociation probability per pulse is unity, is a good estimator of the global fraction of molecules dissociated per pulse:

$$V_{\mathrm{eff}} = \int dV\, f(\Phi). \tag{6}$$

First, the dependence of the remnant fraction of $CDCl_3$, R_F, on the number of irradiation pulses, N_p, and the cell volume, V_{cell}, was determined by FTIR spectrometry. Some of the results obtained are shown in Fig. 6 evidencing that the global fraction of molecules dissociated per pulse increases with the increase of the fluence at the focus, Φ_0. The effective volume of dissociation for the different fluence values was obtained from non-linear regression of the R_F versus N_p curves using

$$R_F = \left(1 - \frac{V_{\mathrm{eff}}}{V_{\mathrm{cell}}}\right)^{N_p}. \tag{7}$$

The dependence of the effective volume of dissociation on the fluence in the range 10–400 J cm^{-2} is shown in Fig. 7. These results were modeled with (8), which results from integrating (6) with the probability of dissociation per pulse defined in (4) and the fluence distribution described in (2) and (3):

$$V_{\mathrm{eff}} = \frac{1}{2} V_R \int_0^{\delta} du\,(u^2+1)\left[1 + \mathrm{erf}\left(\frac{1}{\sqrt{2}\sigma} \ln\left(\frac{\eta_0}{u^2+1}\right)\right)\right] \tag{8}$$

with

$$\delta = \frac{L}{2Z_R} \tag{9}$$

and η_0, the fluence at the focus, Φ_0, to the saturation fluence, Φ_{sat}, ratio, L, the cell length and V_R, the Rayleigh volume defined as

$$V_R = 2\pi Z_R w_0^2. \tag{10}$$

The fit is shown in solid line in Fig. 7 in an extended fluence interval in order to visualize the three different fluence regimes derived from (8) which are also schematized. In regime I, the saturation fluence is never attained in the irradiation volume ($\Phi < \Phi_{\mathrm{sat}}$). In regime II, there is a central region, where the fluence is larger than the saturation fluence ($\Phi > \Phi_{\mathrm{sat}}$), and two regions near the windows within which the saturation fluence is not reached ($\Phi < \Phi_{\mathrm{sat}}$). Finally, region III is characterized by a fluence larger than the saturation fluence in all the irradiation volume ($\Phi > \Phi_{\mathrm{sat}}$). The values of the effective volume measured in this work correspond to the fluence regime II. An excellent agreement between the values of the parameters σ and Φ_{sat} obtained from the deconvolution of the experimental values with the model described by (8) with those resulting from the fluorescence intensity fit was found.

The values of the parameters σ and Φ_{sat} derived from the deconvolution of the fluence dependence of the effective volume data with a probability function described by a

CLNDF coincide within experimental error with those obtained from the fit of the fluence dependence of the fluorescence intensity data with the same probability function. This result, together with the assumption that the observation region in the LIF experiments corresponds to a zone of constant fluence in the fluence regime II, proves that the LIF technique implemented in this work allows the direct determination of the dissociation probability per pulse.

The comparison of the results shown in Figs. 5 and 7 evidences that the LIF technique is much more sensitive than the effective volume technique and enables us to determine the dissociation probability per pulse of small and medium size molecules with high Φ_{sat} values, with less number of irradiating pulses.

4 Conclusions

An irradiation and detection system's geometry which enabled the LIF technique to be used to determine in a direct manner the dissociation probability in tightly focused IRMPD was implemented.

The dependence of the LIF signals of the IRMPD of $CDCl_3$ on fluence in the 3–400 $J\,cm^{-2}$ range was fitted with a Cumulative Log-Normal Distribution Function, and the molecular parameters $\sigma = 0.60 \pm 0.02$ and $\Phi_{sat} = (18 \pm 1)\ J\,cm^{-2}$ were obtained. The resultant value of Φ_{sat} agrees with the values reported by other authors for this molecule in different experimental conditions.

These parameters' values were compared with those derived from the deconvolution of the effective volume obtained from FTIR spectrometry with the Cumulative Log-Normal Distribution Function. The excellent agreement between both methods demonstrates that the LIF technique proves to be a powerful tool to determine the dissociation probability in IRMPD of high dissociation threshold molecules in a much faster manner.

Acknowledgements This research has been supported by the grant ANPCYT, PICT'05 No. 38016 from the Ministerio de Ciencia y Tecnología of Argentina.

References

1. V.S. Letokhov, *Nonlinear Laser Chemistry* (Springer, Berlin, 1983)
2. V.N. Bagratashvili, V.S. Letokhov, *Nonlinear Laser Chemistry* (Springer, Berlin, 1983)
3. V.M. Freytes, J. Codnia, M.L. Azcárate, Appl. Phys. B, Lasers Opt. **103**, 687 (2011)
4. I.P. Herman, Opt. Lett. **4**, 403 (1979)
5. K. Takeuchi, I. Inoue, R. Nakane, Y. Makide, S. Kato, T. Tominaga, J. Chem. Phys. **76**, 398 (1982)
6. G.R. Nicol, D.K. Evans, R.D. McAlpine, Appl. Phys. B, Lasers Opt. **39**, 29 (1986)
7. C. D'Ambrosio, W. Fuss, K.I. Kompa, W.E. Schmidt, J. Opt. Soc. Am. B **5**, 1540 (1988)
8. E. Suzuki, S. Kato, K. Takeuchi, Appl. Opt. **27**, 4445 (1988)
9. S. Kato, K. Takeuchi, Appl. Phys. B **53**, 268 (1991)
10. J.R. Barker, J. Chem. Phys. **72**, 3686 (1980)
11. A.C. Baldwin, J.R. Barker, J. Chem. Phys. **74**, 3813 (1981)
12. A.C. Baldwin, J.R. Barker, J. Chem. Phys. **74**, 3823 (1981)
13. W. Demtröder, *Laser Spectroscopy* (Springer, Berlin, 1998)
14. W. Strube, M. Rossberg, J. Wollbrandt, E. Linke, Rev. Sci. Instrum. **65**, 129 (1994)
15. I.P. Herman, F. Magnotta, R.J. Buss, Y.T. Lee, J. Chem. Phys. **79**, 1789 (1983)
16. T. Shimanouchi, *Tables of Molecular Vibrational Frequencies Consolidated* (1972)
17. F. Magnotta, I.P. Herman, F.T. Aldridge, Chem. Phys. Lett. **92**, 600 (1982)
18. R.D. McAlpine, J.W. Goodale, D.K. Evans, Can. J. Chem. **63**, 2995 (1985)